Journal of Applied Mathematics and Physics, 2023, 11, 1871-1880
https://www.scirp.org/journal/jamp
ISSN Online: 2327-4379
ISSN Print: 2327-4352

Quantum Dynamics via a Hidden Liouville Space

Gombojav O. Ariunbold

Department of Physics and Astronomy, Mississippi State University, Starkville, MS, USA
Email: ag2372@msstate.edu

How to cite this paper: Ariunbold, G.O. (2023) Quantum Dynamics via a Hidden Liouville Space. *Journal of Applied Mathematics and Physics*, **11**, 1871-1880.
https://doi.org/10.4236/jamp.2023.117121

Received: May 29, 2023
Accepted: July 16, 2023
Published: July 19, 2023

Abstract

The traditional simulations may occasionally turn out to be challenging for the quantum dynamics, particularly those governed by the nonlinear Hamiltonians. In this work, we introduce a nonstandard iterative technique where the Liouville space is briefly expanded with an additional (virtual) space only within ultrashort subintervals. This tremendously reduces the cost of time-consuming calculations. We implement our technique for an example of a charged particle in both harmonic and anharmonic potentials. The temporal evolutions of the probability for the particle being in the ground state are obtained numerically and compared to the analytical solutions. We further discuss the physics insight of this technique based on a thought-experiment. Successive processes intrinsically "hitchhiking" via virtual space in discrete ultrashort time duration, are the hallmark of our technique. We believe that this technique has potential for solving numerous problems which often pose a challenge when using the traditional approach based on time-ordered exponentials.

Keywords

Liouville Space, S-Operator, Time-Ordered Exponentials, Quantum Oscillators, Squeezing, Husimi Q-Function

1. Introduction

Although the standard approach based on time-ordered exponentials is extremely useful [1] [2] [3], it may occasionally turn out to be challenging, particularly, in the case of revealing nonlinear quantum dynamics [4] [5] that requires rigorous numerical simulations [6] [7] [8]. Quantum dynamics for arbitrary system are traditionally realized by time evolutions of wave functions in Hilbert space, which can also be expressed in terms of density operators in the Liouville space

[2] [3]. In this work, we introduce a new nonstandard iterative technique formulated as follows. 1) Finite time interval is divided into a large number of discrete subintervals with an ultrashort width. 2) The Liouville space is expanded with an additional (*i.e.*, virtual) space for this ultrashort time duration. The system's original Hamiltonian is, then, modified for the system's space plus virtual space, where the force terms are replaced with the virtual quantum operators. 3) The density operator for the system is extracted by tracing over the virtual operator space. In principle, various virtual operators can be chosen depending on the specific quantum system. Here we choose two-state spin raising and lowering operators because of their simple algebra. In the next section, we present the standard approach using S-operator defined as time-ordered exponentials in Hilbert, and then, in the Liouville space. In Section 3, we introduce our technique and implement it to the well-known example of a charged particle in a harmonic potential. The temporal evolutions of the probability for the particle being in the ground state are obtained by our technique and compared to the analytical solutions obtained using the standard S-operator. By extending this example, we perform numerical simulations for temporal evolutions for the ground state probability for the generalized systems governed by time-dependent nonlinear Hamiltonians. We further discuss the physics insight of this technique based on a thought-experiment, in which a large number of polarized atoms successively interact with a lossless cavity field. The last section is a conclusion.

2. Standard Approach

In this section, the standard approach for quantum dynamics both in Hilbert space and the Liouville space is presented. We consider the system with the Hamiltonian given by

$$\hat{H} = \hat{H}_0 + \hat{V} \tag{1}$$

here $\hat{H}_0$ is the unperturbed (free) and $\hat{V}$ interaction Hamiltonians and we set $\hbar \equiv 1$.

2.1. Quantum Dynamics in Hilbert Space

We begin with the approach for the Hilbert space. In the interaction representation, the rapid state evolution due to $\hat{H}_0$ is removed as

$$\left|\psi_I(t)\right\rangle = \exp\left(i\hat{H}_0 t\right)\left|\psi_S(s)\right\rangle,$$

where $\left|\psi_I(t)\right\rangle$ and $\left|\psi_S(s)\right\rangle$ are wave functions in the interaction and Schrödinger representations, respectively. Unitary transformation of initial state in the interaction picture is given as $\left|\psi_I(t)\right\rangle = \hat{U}(t)\left|\psi_I(0)\right\rangle$, here unitary operator $\hat{U}(t)$ satisfies $\hat{U}(t)^{\dagger}\hat{U}(t) = \hat{1}$ and is expressed as $\hat{U}(t) = \exp\left(i\hat{H}_0 t\right)\exp\left(-i\hat{H}t\right)$. Time evolution of $\hat{U}(t)$ can be derived from $i\partial\hat{U}/\partial t = \hat{V}_I(t)\hat{U}(t)$. The Hamiltonian is in the interaction representation as $\hat{V}_I = \hat{V}_I^{\dagger} = \exp\left(i\hat{H}_0 t\right)\hat{V}\exp\left(-i\hat{H}_0 t\right)$.

Choosing time interval between t_2 and t_1 ($t_1 < t_2$), unitary transformation is expressed as [1]

$$\left|\psi_I(t_2)\right\rangle = \hat{S}(t_2,t_1)\left|\psi_I(t_1)\right\rangle \tag{2}$$

with S-operator $\hat{S}(t_2,t_1)$. We divide time interval $t_2 - t_1$ into N sub-intervals with a width of Δt. At mid-time $\tau_j = t_1 + (j - 1/2)\Delta t$ in the jth interval, the S-operator is written as [1]

$$\hat{S}(\tau_j + \Delta t/2, \tau_j - \Delta t/2) = \mathrm{e}^{-i\hat{V}_I(\tau_j)\Delta t} \tag{3}$$

where $N \to \infty$ and $\Delta t \to 0$ but $t_2 - t_1$ is finite. Equation (3) leads to the traditional time-ordered exponential given as [1]

$$\hat{S}(t_2,t_1) = \hat{T}\left[\prod_{j=1}^{N} \mathrm{e}^{-i\hat{V}_I(\tau_j)\Delta t}\right] = \hat{T}\left[\mathrm{e}^{-i\int_{t_1}^{t_2}\hat{V}_I(t)\mathrm{d}t}\right] \tag{4}$$

where time ordering for boson operators is defined as $\hat{T}\left[\hat{O}_1(\tau_1)\ \hat{O}_2(\tau_2)\ \cdots\ \hat{O}_N(t_N)\right] = \hat{O}_{p_1}(\tau_{p_1})\ \hat{O}_{p_2}(\tau_{p_2})\ \cdots\ \hat{O}_{p_N}(t_{p_N})$ with $\tau_{p_1} > \tau_{p_2} \cdots > \tau_{p_N}$.

2.2. Examples

As an example, we consider a driven harmonic oscillator. For that temporal evolutions of the ground state using S-operator are given in Equation (4). Let a particle of a charge $q \equiv 1$, mass $m \equiv 1/2$ be in a harmonic potential ($\hbar \equiv 1$). The driving electric field is $E(t) \equiv 1$, if $T > t > 0$, and otherwise, it is zero and ω is the frequency of the oscillator. In the interaction picture, the Hamiltonian is written as

$$\hat{V}_I(t) = \hat{R}(t)\varepsilon^*(t) + \hat{R}^\dagger(t)\varepsilon(t) \tag{5}$$

where time-dependent operators are $\hat{R}(t) = \hat{b}(t) = \hat{b}\mathrm{e}^{-i\omega t}$ and $\hat{R}^\dagger(t) = \hat{b}^\dagger(t) = \hat{b}^\dagger \mathrm{e}^{i\omega t}$ and the force terms are $\varepsilon(t) = \varepsilon^*(t) = -\sqrt{1/\omega}E(t)$. The probability $p(T)$ for the particle to remain in the ground state $\left|\psi_0\right\rangle$ after time T is written as

$$p(T) = \left|\left\langle\psi_0\right|\hat{S}(T,0)\left|\psi_0\right\rangle\right|^2 \tag{6}$$

The probability amplitude is given by S-operator from Equation (4) as

$$\left\langle\psi_0\right|\hat{S}(T,0)\left|\psi_0\right\rangle = \left\langle\psi_0\right|\hat{T}\mathrm{e}^{-i\int_0^T \hat{V}_I(t')\mathrm{d}t'}\left|\psi_0\right\rangle = \mathrm{e}^{-iB(T)} \tag{7}$$

where $B(T) = \int_0^T \mathrm{d}t\mathrm{d}t' \varepsilon(t)^* G(t-t')\varepsilon(t')$ and $G(t)$ is the Green's function. For this simple example, the Green's function is well known

$$G(t) = -i\mathrm{e}^{-i\omega t}\theta(t). \tag{8}$$

Therefore, for the particle, its probability to remain in the ground state after time T is analytically found to be as [1]

$$p(T) = \exp\left[-\frac{4}{\omega^2}\sin^2\left(\frac{\omega T}{2}\right)\right] \tag{9}$$

with pulse area ωT.

This example is the simplest case when a linear Hamiltonian is considered. That conveniently ensures to use the well known Green function in Equation (8). However, in general, the Green's functions are mostly unknown and a laborious numerical method is often needed. Next, we consider two more examples that use nonlinear Hamiltonians. The first example for the nonlinear Hamiltonian is a driven anharmonic oscillator. The Hamiltonian is given in the form in Equation (5) [2] where degenerate two-boson nonlinear operators $\hat{R}(t)=\hat{b}^2(t)=\hat{b}^2 e^{-2i\omega t}$ and $\hat{R}^\dagger(t)=\hat{b}^{2\dagger}(t)=\hat{b}^{2\dagger}e^{2i\omega t}$ and the force terms $\varepsilon(t)=\varepsilon^*(t)=-\sqrt{1/2\omega}E(t)$ are assumed to have a similar form as in the harmonic oscillator case. The second example for the nonlinear Hamiltonian is a driven intensity-dependent oscillator. The Hamiltonian is given in the form in Equation (5) [9] with the intensity-dependent nonlinear boson operators $\hat{R}(t)=\hat{b}(t)\sqrt{\hat{b}^\dagger\hat{b}}$ and $\hat{R}^\dagger(t)=\sqrt{\hat{b}^\dagger\hat{b}}\hat{b}^\dagger(t)$ and $\varepsilon(t)$ is assumed to be the same as before. In Section 3, we numerically solve for the probability time evolutions for these nonlinear systems and compare with the approximate analytical results.

3. Nonstandard Approach

3.1. Quantum Dynamics in Liouville Space

Before introducing our technique, let us first replace the wave functions in Hilbert space with density operators in Liouville space [2] [3]. We recall that $\rho_N \equiv \rho(t_2)=|\psi_I(t_2)\rangle\langle\psi_I(t_2)|$ and $\rho_0 \equiv \rho(t_1)=|\psi_I(t_1)\rangle\langle\psi_I(t_1)|$ from Equation (2). Using S-operator in the jth interval from Equation (3), we rewrite Equation (2) in terms of density operators rather than wave functions as

$$\hat{\rho}_j = e^{-i\hat{V}_I(\tau_j)\Delta t}\hat{\rho}_{j-1}e^{i\hat{V}_I(\tau_j)\Delta t} \tag{10}$$

here $\hat{\rho}_j=\hat{\rho}(\tau_j+\Delta t/2)$ and $\hat{\rho}_{j-1}=\hat{\rho}(\tau_j-\Delta t/2)$. In the traditional approach, to obtain $\hat{\rho}(t_2)$ at later time t_2 for any given initial state $\hat{\rho}(t_1)$ at t_1 Equation (10) is repeatedly evaluated, where $\Delta t \ll 1$ and $N \gg 1$ but $t_2-t_1=N\Delta t$ is finite. It is also important to note that Equation (10) is the formal solution of the Liouville-von Neumann equation [2].

3.2. Quantum Dynamics in Liouville Space Restructured with a Virtual Space

From this point, we implement our new nonstandard approach, rather directly evaluating Equation (10). As before, finite time interval t_2-t_1 is divided into N discrete subintervals with an ultrashort width of Δt. The Liouville space is expanded with a two-state spin operator space for duration of Δt. The system's original Hamiltonian is, then, modified for the system's space plus spin space, where the force terms are replaced with the spin operators. The density operator for the system is extracted by tracing over the spin operator space. In the jth interval with an infinitesimally short width of Δt, it is an acceptable ansatz where we replace the original Hamiltonian $\hat{V}_I(\tau_j)$ by new Hamiltonian expanding it

with an additional virtual space $\hat{A}_j$ as

$$\hat{V}_I(\tau_j) \to \hat{V}_I(\tau_j) \otimes \hat{A}_j \tag{11}$$

where $\left[\hat{V}_I(\tau_j), \hat{A}_j\right] = \hat{0}$. For the sake of simplicity, $\hat{A}_j$ can be chosen to be a two-state spin operator defined as

$$\hat{A}_j = |\alpha_j|^2 |\uparrow\rangle\langle\uparrow| + \alpha_j^* \beta_j |\downarrow\rangle\langle\uparrow| + \alpha_j \beta_j^* |\uparrow\rangle\langle\downarrow| + |\beta_j|^2 |\downarrow\rangle\langle\downarrow| \tag{12}$$

with $|\alpha_j|^2 + |\beta_j|^2 = 1$. For this choice, the force terms are replaced with the raising $|\uparrow\rangle\langle\downarrow|$ and lowering $|\downarrow\rangle\langle\uparrow|$ operators specifically as

$$\begin{aligned} \varepsilon(\tau_j) e^{i\omega\tau_j} &\to \eta_j \alpha_j \beta_j^* |\downarrow\rangle\langle\uparrow| \\ \varepsilon^*(\tau_j) e^{-i\omega\tau_j} &\to \eta_j^* \alpha_j^* \beta_j |\uparrow\rangle\langle\downarrow| \end{aligned} \tag{13}$$

Thus, in the jth interval with Δt width, this original Hamiltonian Equation (5) can be replaced with a new Hamiltonian $\hat{V}_A(\tau_j)$, also known as the unified Jaynes-Cummings Hamiltonian [10] [11] as

$$\hat{V}_A(\tau_j) = \eta_j^* \hat{R}(\tau_j) |\uparrow\rangle\langle\downarrow| + \eta_j \hat{R}^\dagger(\tau_j) |\downarrow\rangle\langle\uparrow|. \tag{14}$$

Instead of the original approach given by Equation (10) for $\hat{\rho}_j$, we introduce an iterative relation for new density operator ρ_j using the modified Hamiltonian given in Equation (14) as

$$\hat{\varrho}_j = \mathrm{Tr}_A \left[e^{-i\hat{V}_A(\tau_j)\Delta t} \hat{A}_j \otimes \hat{\varrho}_{j-1} e^{i\hat{V}_A(\tau_j)\Delta t} \right] \tag{15}$$

Therefore, our goal is to demonstrate that the two density operators converge

$$\hat{\varrho}_N \simeq \hat{\rho}_N \tag{16}$$

for the same pure initial state.

3.3. A Thought-Experiment

The essentials of our iterative technique are explained by the following thought-experiment. As sketched in Figure 1, let us consider a monokinetic beam consisting of individual two-level atoms. Each atom is prepared in arbitrary coherent superposition of the upper and lower states [8] [12] [13]. The atoms are then injected into a lossless cavity in a well controlled rate where only one atom at a time is present inside the cavity for duration Δt. At the exit from the cavity

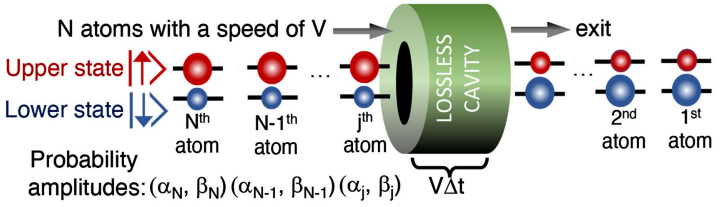

Figure 1. A monokinetic beam of N two-level atoms passing through a lossless cavity. Each atom interacts with the cavity field for a duration of Δt. The cavity field builds up to its final state $\hat{\varrho}_N$ (or $|\psi_I(t)\rangle$) from initial state $\hat{\varrho}_0$ (or $|\psi_I(0)\rangle$) after a finite time $t = N\Delta t$.

the individual atoms are not intended to be measured. Total number of atoms is N and the jth atom-field coupling constant is η_j. Although the present model can be generalized to multi-level atoms [8] [9] [14], for the sake of simplicity, we consider only two-level atoms, where $|\uparrow\rangle$ and $|\downarrow\rangle$ are upper and lower atomic states, respectively. Correspondingly, α_j and β_j are probability amplitudes for the jth atomic upper and lower states. Thus, as a result of numerically solving Equation (15), the final cavity field state is evaluated from the existing initial quantum state in the cavity after time $t = \Delta t N$. For example, when atoms are prepared in the same phase then the cavity field evolves to the so-called superradiant state [5] [8] [15] [16] [17] [18]. The mean number of photons created in the cavity (*i.e.*, field intensity) is proportional to N^2 rather than N. On the other hand, when each successive pair of atoms are prepared in perfectly out-of-phase, then the cavity field evolves to the sub-radiant state [5] [8]. Moreover, we justify that time evolutions involve pure states after tracing over the virtual space operator. As demonstrated in our earlier work [8], an initial coherent state given as $|\gamma_0\rangle$ evolves into $|\gamma(t)\rangle \simeq |\gamma_A + \gamma_0\rangle$, with $\gamma_A = -i\eta\alpha\beta^* t$ at later time t. Therefore, the above statement that our technique maintains time evolutions for pure states is justified not only for infinitesimally short Δt interval, but also for finite time t.

3.4. Examples

Here we employ our technique for the previous example for a charged particle in harmonic potential. We evaluate Equation (15) using the Hamiltonian given in Equation (14) both numerically and analytically, however, for the sake of simplicity, only for initial vacuum state. Thus, the modified Hamiltonian $\hat{V}_A(\tau_j)$ in Equation (14) is written in terms of $\hat{R}(t) \equiv \hat{b}(t)$. Comparing the Hamiltonian in Equation (5) with the ansatz in Equation (13), we obtain $\varepsilon(\tau_j)\mathrm{e}^{i\omega\tau_j} = -\eta_j\alpha_j\beta_j^* = -\eta_j\zeta_j^*$. The parameter $\zeta_j = \alpha_j^*\beta_j$ stands for a coherence between spin states. For example, for parameters chosen to be as $\eta_j = 1$, $|\alpha_j| = |\beta_j| = 1/\sqrt{2}$, it is given by $-\mathrm{e}^{i\omega\tau_j}/2$ with $|\zeta_j| = 1/2$. In the Fock state representation, the jth density matrix elements are $\rho_j(n,n') = \langle n|\hat{\rho}_j|n'\rangle$. We numerically evaluate $\varrho_N(n,n')$ from Equation (15), to obtain $\varrho_N(0,0)$, at $t_2 - t_1 = T$ with $t_1 = 0$ to compare the probability $p(T)$ given in Equation (9). Equation (9) is rewritten in terms of time-independent parameters $\eta_j = 1$, $|\zeta_j| = |\zeta|$ associated to the virtual operator space as

$$p(T) = \exp\left[-\frac{4|\zeta|^2}{\omega^2}\sin^2\left(\frac{\omega T}{2}\right)\right] \tag{17}$$

In **Figure 2**, the density matrix elements for $\rho_N(0,0)$ (red circles) and $p(t)$ (black curves) are plotted as functions of pulse area per π, $\omega t/\pi$. For the plots in **Figure 2(a)** and **Figure 3(a)**, the parameters include coherence $\zeta = 1/2$, total number $N = 3750$, width of the subintervals $\Delta t = 0.001$, time $T = N\Delta t = 3.75$ frequency $\omega = 2\pi/5$. For the plot in **Figure 2(a')**, except for the larger total

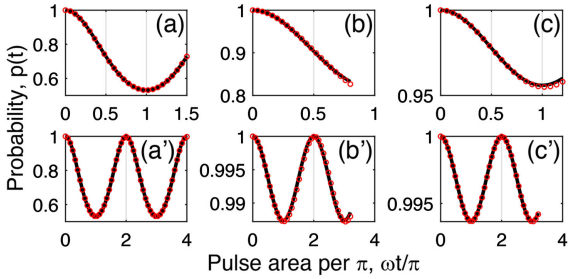

Figure 2. Analytical (black curves) and numerical (red circles) results for temporal evolutions of the probability $p(t)$ for a charged particle driving by the external field being in the ground state as functions of $\omega t/\pi$. Left column: The system with a linear Hamiltonian. Middle column: The system with the degenerate two-boson Hamiltonian. Right column: The system with the intensity-dependent Hamiltonian.

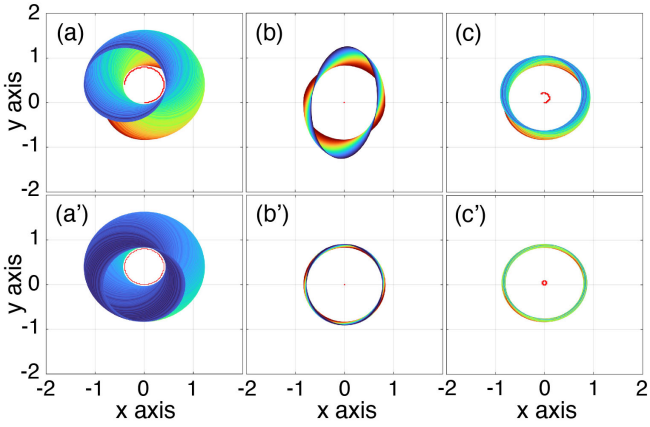

Figure 3. Realizations of dynamics of quantum states from initial vacuum. Numerical calculations of the temporal evolutions displayed by the contour plots of the Husimi Q-functions accompanied with the trajectories (red curves) of the centers of these contours. Left column: The system with a linear Hamiltonian. Middle column: The system with the degenerate two-boson Hamiltonian. Right column: The system with the intensity-dependent Hamiltonian. All parameters are the same as used in **Figure 2**.

number $N=10000$ and later time $T=10$, the rest of parameters remain the same as that given in **Figure 1(a)**. In **Figure 3**, the quasi-distributions given by the Husimi Q-functions are plotted. The Husimi Q-function [2] [4] [5] is defined as $Q(x,y)=\langle\alpha|\hat{\varrho}_N|\alpha\rangle/\pi$, here $\alpha=\sqrt{x^2+y^2}\exp\left[i\operatorname{atan}(y/x)\right]$. Because of coherent state representations, the Q-functions conveniently illustrate the coherent state as a displaced vacuum state with a perfect ring shape [8], preserved for entire time. In **Figure 3**, the red curves indicate the trajectories of displacements of the initial coherent state over time. These trajectories are the centers of single selected contour plots with the fixed value of the Q-functions at any given time *t*. For example, in **Figure 3(a)**, this trajectory follows a circle but is not yet complete circle opposite to that case in **Figure 3(a')**. The parameters used for the plots in **Figures 3(a)-(c)** and **Figures 3(a')-(c')** are the same as those used in **Figures 2(a)-(c)** and **Figures 2(a')-(c')**, respectively. In **Figure 2(b)** and **Figure 2(b')** and **Figure 2(c)** and **Figure 2(c')**, the realizations of quantum dynamics

for nonlinear Hamiltonians with $\hat{R}(t)=\hat{b}^2(t)$ in (b, b') representing two-boson processes and $\hat{R}(t)=\hat{b}(t)\sqrt{\hat{b}^{\dagger}\hat{b}}$ in (c, c') representing intensity-dependent processes are demonstrated. Similar to **Figure 2**, the numerical results for $\varrho_N(0,0)$ are compared to approximate analytical expressions for time evolutions for the probabilities being in the ground state $p(T)$ after time T in **Figure 3(b)** and **Figure 3(c)**. In the case of two-boson transition processes, the approximate analytical expressions are obtained to be

$$p(T)\approx\exp\left[-\frac{8|\zeta|^2}{\omega^2}\sin^2\left(\frac{\omega T}{2}\right)\right] \tag{18}$$

For **Figure 2(b)** and **Figure 2(c)**, the parameters are given as $N=8000$, $\Delta t=0.0001$, $T=0.8$, $\omega=\pi$ and $\omega T/\pi=0.8$, while for **Figure 2(b')** and **Figure 2(c')**, the parameters are the same as in (b) except for frequency $\omega=4\pi$ and, thus, $\omega T/\pi=3.2$. In **Figure 3(b)**, the Q-functions display how the initial vacuum state with a ring shape is transformed to the significantly squeezed states with its signature oval shape [2] [8] [19] [20] for a slower process with a frequency of $\omega=\pi$. However, for the fast process with $\omega=4\pi$, the state remains merely in vacuum state without observable squeezing. Lastly, **Figure 2(c)** and **Figure 2(c')** and **Figure 3(c)** and **Figure 3(c')** represent the temporal evolutions for the Holstein-Primakoff $\mathrm{SU}(1,1)$ transformed states [9] [21]. Similarly, the probabilities for slow (**Figure 2(c)**) versus fast (**Figure 2(c')**) processes are compared. It is important to note that the analytical formula for the probability for these processes is identical to Equation (17). However, the deviation (*i.e.*, displacement) is not as much pronounced as for coherent states (see, **Figure 3(c)** and **Figure 3(c')**).

4. Conclusions

In the standard approach, quantum dynamics for arbitrary system are realized by the time evolutions of wave functions in Hilbert space, which can also be expressed in terms of density operators in Liouville space. However, the standard quantum simulations may occasionally turn out to be challenging, particularly, for nonlinear dynamical systems.

In this work, we introduce a new nonstandard iterative technique, formulated as follows. 1) A finite time interval is divided into a large number of discrete subintervals with an ultrashort width. 2) The Liouville space is synthesized with an additional virtual space for ultrashort time duration and the quantum system's original Hamiltonian is modified accordingly. In particular, the force terms are replaced with virtual quantum operators. 3) The density operator for the system is extracted by tracing over the virtual operator space. In principle, various virtual operators can be chosen depending on specific quantum system. For example, the simple algebra of using two-state spin raising and lowering operators reduces the cost of time-consuming calculations. After introducing our technique, we implement it to the well-known example of a charged particle in a

harmonic potential. Temporal evolutions of the probability for the particle being in the ground state are obtained by the present technique and compared to the analytical solutions given by the standard approach. We further discuss the physics insight of this technique based on a thought-experiment. Lastly, we perform numerical simulations for temporal evolutions for the ground state probability for generalized systems governed by the time-dependent nonlinear Hamiltonians. The quantum dynamics are realized by using the quasi-distributions.

Successive processes implicitly "hitchhiking" via virtual space for discrete ultrashort time duration, are the hallmark of our technique. We believe that this novel technique has potential for solving numerous problems otherwise challenging to address using the standard approach based on time-ordered exponentials.

Conflicts of Interest

The author declares no conflicts of interest regarding the publication of this paper.

References

[1] Coleman, P. (2015) Introduction to Many-Body Physics. Cambridge University Press, Cambridge. https://doi.org/10.1017/CBO9781139020916

[2] Scully, M. and Zubairy, S. (1997) Quantum Optics. Cambridge University Press, Cambridge. https://doi.org/10.1017/CBO9780511813993

[3] Mukamel, S. (1995) Principles of Nonlinear Optical Spectroscopy. Oxford University Press, Oxford.

[4] Perina, J. (1991) Quantum Statistics of Linear and Nonlinear Optical Phenomena, 2nd Edition, Kluwer, Dordrecht. https://doi.org/10.1007/978-94-011-2400-3

[5] Mandel, L. and Wolf, E. (1995) Optical Coherence and Quantum Optics. Cambridge University Press, Cambridge. https://doi.org/10.1017/CBO9781139644105

[6] Fisher, R.A., Nieto, M.M. and Sandberg, V.D. (1984) Impossibility of Naively Generalizing Squeezed Coherent States. *Physical Reviews D*, **29**, 1107-1110. https://doi.org/10.1103/PhysRevD.29.1107

[7] Braunstein, S.L. and McLachlan, R.I. (1987) Generalized Squeezing. *Physical Reviews A*, **35**, 1659-1667. https://doi.org/10.1103/PhysRevA.35.1659

[8] Ariunbold, G., Perina, J. and Gantsog, T. (1999) Nonclassical States in Cavity with Injected Atoms. *Journal of Optics B*: *Quantum Semiclassical Optics*, **1**, 219-224. https://doi.org/10.1088/1464-4266/1/2/004

[9] Ariunbold, G. and Perina, J. (1998) Holsttein-Primakoff *SU*(1,1) Coherent State in Micromaser Under Intensity Dependent Janynes-Cummings Interaction. *Acta Physica Slovaca*, **48**, 315-322. http://www.physics.sk/aps/pubs/1998/aps_1998_48_3_315.pdf

[10] Bonatsos, D., Daskaloyannis, C. and Lalassisis, G.A. (1993) Unification of Jaynes-Cummings Models. *Physical Review A*, **47**, 3448-3451. https://doi.org/10.1103/PhysRevA.47.3448

[11] Shanta, P., Chaturvedi, S., Srinivasan, V. and Jagannathan, R. (1994) Unified Approach to the Analogues of Single-Photon and Multiphoton Cohernet States for

Generalized Bosonic Oscillators. *Journal of Physics A*: *Mathematical and General*, **27**, 6433-6442. https://doi.org/10.1088/0305-4470/27/19/016

[12] Meschede, D., Walther, H. and Müller, G. (1985) One-Atom Maser. *Physical Review Letters*, **54**, 551-554. https://doi.org/10.1103/PhysRevLett.54.551

[13] Kien, F.L., Scully, M.O. and Walther, H. (1993) Generation of a Coherent State of the Micromaser Field. *Foundation of Physics*, **23**, 177-184. https://doi.org/10.1007/BF01883622

[14] Ariunbold, G., Perina, J., Gantsog, T. and El-Orany, F.A.A. (1999) Two-Mode Correlated States in Cavity with Injected Atoms. *Acta Physica Slovaca*, **49**, 627-632. http://www.physics.sk/aps/pubs/1999/aps-1999-49-4-627.ps

[15] Dicke, R.H. (1954) Coherence in Spontaneous Radiation Processes. *Physical Review*, **93**, 99-110. https://doi.org/10.1103/PhysRev.93.99

[16] Benedict, M.G. (1995) Super-Radiance: Multiatomic Coherent Emission. CRC Press, London.

[17] Ariunbold, G.O. (2022) A Cascade Superradiance Model. *Physics Letters A*, **452**, Article ID: 128468. https://doi.org/10.1016/j.physleta.2022.128468

[18] Ariunbold, G.O., Sautenkov, V.A., Li, H., Murawski, R.K., Wang, X., Zhi, M., Begzjav, T., Sokolov, A.V., Scully, M.O. and Rostovtsev, Y.V. (2022) Observations of Ultrafast Superfluorescent Beatings in a Cesium Vapor Excited by Femtosecond Laser Pulses. *Physics Letters A*, **428**, Article ID: 127945. https://doi.org/10.1016/j.physleta.2022.127945

[19] Yuen, H.P. (1976) Two-Photon Coherent States of the Radiation Field. *Physical Review A*, **13**, 2226-2243. https://doi.org/10.1103/PhysRevA.13.2226

[20] Stoler, D. (1970) Equivalence Classes of Minimum Uncertainty Packets. *Physical Review D*, **1**, 3217-3219. https://doi.org/10.1103/PhysRevD.1.3217

[21] Holstein, T. and Primakoff, H. (1940) Field Dependence of the Intrinsic Domain Magnetization of a Ferromagnet. *Physical Review*, **58**, 1098-1113. https://doi.org/10.1103/PhysRev.58.1098